LETTERS IN BIOMATHEMATICS
An International Journal

Intercollegiate Biomathematics Alliance

RESEARCH ARTICLE

OPEN ACCESS

A Hybrid Differential Equations Model for the Dynamics of Single and Double Strand Breaks of Cancer Cells Treated by Radiotherapy: A Definition for Tumor Life-Span

Shantia Yarahmadian[a], Amin Oroji[b], Anna Katherine Williams[a]

[a] Mississippi State University; [b] University of Malaya

ABSTRACT

According to the Target Theory, the tumor population is divided into multiple different subpopulations, called targets, based on the diverse effects of ionizing radiation on human cells. Radiation particles can cause single or double-strand break(s). As such, cells are divided into three subpopulations, namely cells with no DNA fragmentation, cells with DNA single-strand breaks, and cells with DNA double-strand breaks. This work introduces a hybrid differential equation model, with coefficients described by random variables representing transition rates between targets. The model is utilized to simulate the dynamics of targets and describes the cell damage heterogeneity and the repair mechanism between two consecutive dose fractions. Therefore, a new definition of tumor lifespan based on population size is achieved. Stability and bifurcation analysis are performed. Finally, the probability of target inactivity after radiation and the probability of target re-activation following the repair mechanism are evaluated with respect to the tumor lifespan.

ARTICLE HISTORY
Received October 22, 2021
Accepted July 20, 2022

KEYWORDS
Radiotherapy, Cancer, Differential Equations, Target Theory, Single-Strand breaks, Double-Strand breaks

1 Introduction

Cancer affects millions of people in the world, and the appearance of mathematical modeling in cancer research has steadily increased over time. Multidisciplinary collaboration is essential in cancer research, and mathematical applications significantly contribute to many areas of cancer research by providing a deeper insight and establishing a framework for understanding properties of cancer cells.

Radiation therapy (RT) is one of the most common methods of cancer treatment. Modeling the effects of radiation on cancer cells is one of the most challenging areas in mathematical biology and by applying the Target theory and DNA fragmentations, a variety of models have been created to describe the influence of radiation on tumor cells.

There exists a vast literature on mathematical models proposed for the population dynamics of tumors and the tumor growth. Among them, we refer reader to review articles Araujo and McElwain (2004); Bellomo and Preziosi (2000); Bellomo et al. (2008); Byrne et al. (2006); Martins et al. (2007); Nagy (2005); Roose et al. (2007); Chaplain (2008); Oroji et al. (2016). Partial Differential Equations (PDEs) are one of the most popular methods to describe spatial models. Many different PDE models are proposed for tumor growth. Among them, we refer the reader to Araujo and McElwain (2004); Roose et al. (2007); Chaplain (2008).

Mathematical models based on kinetic theory are known as the second class of mathematical models for tumor growth (Bellomo and Delitala, 2008). The other important class of models for the population dynamics of tumor cells and tumor growth are Ordinary Differential Equations (ODEs) models, which are used to describe non-spatial models (Adam and Bellomo, 2012; Dullens et al., 1986; Bajzer et al., 1996; Sachs et al., 2001; Nagy, 2005). These models contain a simple and intuitive structure, and they are able to explain the interaction between tumor cells with each other, tumor cells and normal tissues, and the response of tumor cells to the different treatments (Bajzer et al., 1996; Sachs et al., 2001). ODE models can be classified based on the compartments of the model (e.g., one compartment Gompertz, 1825; two Sachs et al., 2001; three Bajzer et al., 1996; six or more compartments Piantadosi et al., 1983). The other models focus on the practical features of the tumor growth (Nagy, 2005).

CONTACT Shantia Yarahmadian syarahmadian@math.msstate.edu

The earliest models for the fractionated radiation therapy were developed based on the Target theory, Hit theory (Cohen, 1971), and Power Law equation of the Nominal Standard Dose theory of fractionated cells (Ellis, 1969). In fractionated radiotherapy, radiotherapy is applied in a number of doses called fractions given in a period of time. Target theory is associated to ionization of cells during the process of radiotherapy and Hit theory is based on the idea that there are sensitive targets in the cell that can go through ionization during radiotherapy, which is called a hit event. The novelty of the current work is in including cell damage heterogeneity and the repair mechanism between two consecutive RT dose fractions by considering single and double strand DNA breaks. Ionizing radiation not only causes Double-Strand Breaks (DSBs) but also causes a substantial extent of DNA base lesions, which are called Single-Strand Breaks (SSBs) (Khoronenkova and Dianov, 2015; Vilenchik and Knudson, 2000). One Gray of irradiation will produce approximately 10^5 ionizations, 1000 DNA base damages, 1000 single-strand DNA breaks (SSBs), and 20 to 40 double-strand DNA breaks (DSBs) (Joiner and van der Kogel, 2009). Specialized repair systems have consequently developed to detect and repair base damage, e.g., base excision repair (BER), and single-strand breaks, or single-strand break repair (SSBR). SSBR is closely associated with BER. Single-strand breaks can result in DSB development in two ways. In the first way, ionizing radiation damage frequently takes place in groups, and subsequently, a number of SSBs will also exhibit damage to neighboring DNA bases. During base damage, repair via BER, SSBs forms temporarily. Upon the occurrence of a strand opposite to a radiation-induced SSB incurring base damage, the temporarily created break during BER may join the radiation break on the opposite strand, which results in a DSB.

The second way happens if a SSB has come upon a replication fork in the S phase, and if the fork and single-ended DSB will disintegrate (Joiner and van der Kogel, 2009). Mutations, genomic instability, and cell death may result from failing to mend DNA breaks like DSBs. Due to the critical effects of DSBs, cells have developed homologous recombination (HR) and non-homologous end joining (NHEJ) as two principal repair mechanisms (Ohnishi et al., 2009). In the course of HR, a double-strand break may transform into a single strand break because the single-strand DNA production is essential for HR (Joiner and van der Kogel, 2009).

As target and hit theories play the central role in radiotherapy, therefore in this work, we study the significance of including single and double strand breaks in the treatment by radiotherapy to be able to understand the effectiveness of the treatment. As such, we propose a tumor population dynamics model via a system of ordinary differential equations with coefficients represented by random variables representing transition rates. Then, we evaluate these transition rates using a Markov chain. Based on the effect of radiation, cells are divided into three subpopulations, which are cells with no effect (x_0), cells with single-strand breaks (x_1), and cells with double-strand breaks (x_2). We analyze the system and its stability numerically. In addition, we have studied the bifurcation of the system with respect to the two parameters, q and r, where q represent the probability of a target deactivation after a dose fraction and r shows a target revival probability between two conservative doses.

The paper is organized as follows: Section 2 introduces the general theory and preliminary findings. The tumor growth model is discussed in terms of a system of ordinary differential equations with Markov chain coefficients. In Section 3, the model is probed with two and three subpopulations based on the DNA fragmentation. Then, the system stability and numerical system bifurcation is studied. A discussion and a comparison with previous studies in the literature are presented in Section 4. Finally, Section 5 concludes the study.

2 Assumptions and Modeling

2.1 Assumptions

The following assumptions are adopted in our modeling framework (Oroji et al., 2018):

1. Cells act independently but they have the same phenotype.

2. The magnitude of each dose fraction (u_0) is considered constant during treatment by RT (i.e., $u_0 = 2\ Gy$). The time-lag of two consecutive dose fractions is 24 hours.

3. It is assumed that each cell consists of m targets. Targets may be deactivated with probability q after each dose fraction. $\mathbf{P} = [p_{ij}]$ describes the treatment probability matrix elements in the transition from i to j inactive targets, i.e., deactivating j targets when i targets were disabled before that (Keinj et al., 2011). This probability matrix is written as

$$\mathbf{P} = [p_{ij}] = \begin{cases} \binom{m-i}{j-i} q^{j-i} (1-q)^{m-j} & \text{if } i \le j, \\ 0 & \text{if } j < i. \end{cases} \tag{2.1}$$

4. The revival probability for an inactive target during the period between two consecutive fractions is r. It is assumed that targets can be repaired independent from each other. As such, $\mathbf{R} = [r_{ij}]$ describes the repair probability matrix in the

transition from i to j, where $i-j$ targets among the i inactive targets are considered to be repaired (Keinj et al., 2011):

$$\mathbf{R} = [r_{ij}] = \begin{cases} \binom{i}{j} r^{i-j}(1-r)^j & \text{if } j \le i < m, \\ 0 & \text{if } i < j, \end{cases} \tag{2.2}$$

where $r_{mm} = 1$ and $r_{mj} = 0$ for $m \neq j$.

5. Cells can reproduce if all targets become active. For simplicity, we assume that just before the repair mechanism acts, cells in subpopulation x_0 can give birth to new cells proportional to subpopulation x_0 with a constant rate of $\mu(1-q)^m$. As such, each cell in subpopulation x_0 can divide into exactly two daughter cells with probability μ or it can remain unchanged with probability $(1-\mu)$ between two consecutive dose fractions.

6. Tumor lifespan is defined as the minimum necessary dose fractions for the elimination the entire tumor. If $N(t)$ represents the total target population in the tumor then the tumor lifespan is described by the following (Oroji et al., 2016):

$$L = \min\{\, \lfloor t \rfloor : \lfloor N(t) \rfloor = 0 \,\}, \tag{2.3}$$

where, e.g., $\lfloor t \rfloor$ is the greatest integer less than or equal to t.

7. Following Keinj et al. (2011), the dynamic of the involved Markov chain is characterized by matrix $\Pi = [\pi_{ij}]$, which takes the effect of dose fractions first and then the repair. Therefore, $\Pi = PR$.

2.2 Model

Based on the assumption considered in Section 2.1, the proposed model is written as follows (Oroji et al., 2018). In our model, each cell has m targets. In the numerical simulations, there are three targets, x_0, x_1 and x_2. x_0 represents the population of not being affected by radiation, x_1 having single strand breaks (SSB) and x_2 having double strand breaks (DSB). Each targets can be deactivated with probability q after each dose fraction. Each target can be revived with probability r.

$$\begin{cases} \dfrac{dx_0(t)}{dt} = [\pi_{0,0} + \mu(1-q)^m - 1]x_0(t) + \displaystyle\sum_{i=1}^{m-1} \pi_{i,0}x_i(t) \\ \dfrac{dx_1(t)}{dt} = [\pi_{1,1} - 1]x_1(t) + \displaystyle\sum_{\substack{i=0 \\ i\neq 1}}^{m-1} \pi_{i,1}x_i(t) \\ \qquad\vdots \\ \dfrac{dx_{m-1}(t)}{dt} = [\pi_{m-1,m-1} - 1]x_{m-1}(t) + \displaystyle\sum_{i=0}^{m-2} \pi_{i,m-1}x_i(t) \end{cases} \tag{2.4}$$

with initial conditions $\mathrm{x}(0) = (n_0, 0, \ldots, 0)^\top$. Here, $\pi_{i,j}$ represents the transition probability from the state $x(i)$ to $x(j)$. In the matrix form, System (2.4) can be rewritten as

$$\dot{x}(t) = A(q,r)\, x(t) \tag{2.5}$$

where matrix A is defined as

$$A = [a_{ij}] = \begin{cases} \pi_{0,0} + \mu(1-q)^m - 1 & \text{if } i = j = 1, \\ \pi_{i,i} - 1 & \text{if } i = j \neq 0, \\ \pi_{j,i} & \text{if } i \neq j. \end{cases} \tag{2.6}$$

3 Simulation and Results

3.1 Cells with single-strand breaks and double-strand breaks as two subpopulations

In applying a dose fraction, a realistic scenario is cells having only four possibilities: not being affected by radiation particles (cells in subpopulation x_0), incurring Single-Strand Breaks (SSB) (cells in subpopulation x_1), incurring Double-Strand Breaks (DSB) (cells in subpopulation x_2), or dying. In this regard, we study a system with three targets, $m = 3$. We study the stability of the zero solution and establish the necessary conditions for this stability. Then we report the numerical simulation results. These results can characterize the effectiveness of the RT treatment.

3.1.1 Stability analysis

We examine the stability of the System (2.4) for the parameter value $\mu = 1$. We have used numerical simulations for verifying the necessary stability conditions. In this case, System (2.4) is reduced to

$$\begin{cases} \dfrac{dx_0(t)}{dt} = [\pi_{0,0} + (1-q)^3 - 1]x_0(t) + \pi_{1,0}x_1(t) + \pi_{2,0}x_2(t) \\ \dfrac{dx_1(t)}{dt} = \pi_{0,1}x_0(t) + [\pi_{1,1} - 1]x_1(t) + \pi_{2,1}x_2(t) \\ \dfrac{dx_2(t)}{dt} = \pi_{0,2}x_0(t) + \pi_{1,2})x_1(t) + [\pi_{2,2} - 1]x_2(t) \end{cases} \tag{3.1}$$

with the initial condition $\mathrm{x}(0) = (n_0, 0, 0)$. Now, suppose that A denotes the coefficient matrix of System (3.1), which is written as follows:

$$A(q,r) = \begin{bmatrix} [3qr(q-1)^2 - 2(q-1)^3 - 3q^2r^2(q-1)] - 1 & r(q-1)^2 - 2qr^2(q-1) & -r^2(q-1) \\ 3q^2r(2r-2)(q-1) - 3q(q-1)^2(r-1) & [2qr(2r-2)(q-1) - (q-1)^2(r-1)] - 1 & r(2r-2)(q-1) \\ -3q^2(q-1)(r-1)^2 & -2q(q-1)(r-1)^2 & -[(q-1)(r-1)^2] - 1 \end{bmatrix}.$$

Theorem 3.1. *System (3.1) has only one equilibrium point at the origin if* $0 < r < 1$, $q = 0.5$ *and* $\mu = 1$.

Proof. Substituting $q = 0.5$ in the matrix and evaluating its determinant results in $\det(A) = \frac{9(r-1)}{32}$, which is nonzero for $0 < r < 1$. □

Remark 3.1 (Routh-Hurwitz criterion). *Routh-Hurwitz criterion is necessary and sufficient condition for a matrix to have strictly eigenvalues with the negative real parts. This condition forces the linear system with constant coefficients* $X'(t) = AX(t)$ *be asymptotically stable at the origin provided that* $\det(A) \neq 0$. *If the characteristic polynomial of A is*

$$p(\lambda) = \det(A - \lambda I) = \lambda^n + a_1\lambda^{n-1} + a_2\lambda^{n-2} + \cdots + a_n,$$

then the necessary and sufficient condition for stability in the case of $n = 3$ *is* $a_3 > 0$, $a_1 > 0$, *and* $a_1a_2 > a_3$. *For the general case we refer the readers to Coppel (1965, p. 158).*

Theorem 3.2 (Stability result). *System (3.1) is stable at the origin for* $0 < r < 1$, $q = 0.5$ *and* $\mu = 1$.

Proof. Let $P(\lambda)$ be the characteristic polynomial of matrix A. By using the Routh-Hurwitz criterion, System (3.1) is stable if and only if

$$a_1 > 0, \qquad a_3 > 0, \qquad a_1a_2 > a_3 \tag{3.2}$$

where a_1, a_2 and a_3 are the corresponding coefficients of the characteristic polynomial of matrix A, i.e.,

$$P(\lambda) = \lambda^3 + a_1\lambda^2 + a_2\lambda + a_3 \tag{3.3}$$

For $q = 0.5$, the characteristic polynomial of matrix A is written as

$$P(\lambda) = \lambda^3 + \frac{1}{8}(r^2 - r + 4)\lambda^2 + \frac{1}{32}(-r^3 + 7r^2 - 16r + 42)\lambda + \frac{9}{32}(1-r). \tag{3.4}$$

It is clear that $a_1 > 0$ and $a_3 > 0$. Therefore, it is sufficient to show that $a_1a_2 > a_3$ for $0 < r < 1$. By considering

$$g(r) = a_1a_2 - a_3 = \frac{1}{256}(-r^5 + 8r^4 - 39r^3 + 170r^2 - 226r + 600) \tag{3.5}$$

it can be verified that $g(r) > 0$ for $0 < r < 1$ (see Figure 1a). Therefore, the Routh–Hurwitz criterion is satisfied. □

Theorem 3.3. *For* $q < 0.5$, *there exists* $0 < r < 1$, *such that System (3.1) is unstable at the equilibrium point* $(0, 0, 0)$.

Proof. Suppose that $h > 0$ is an arbitrary real number. Corresponding to $q = 0.5 - h$ and $r = 1 - h$,

$$P(\lambda) = \lambda^3 + a_1\lambda^2 + a_2\lambda + a_3 \tag{3.6}$$

represents the characteristic polynomial of the coefficient matrix in System (3.1), where

$$a_3 = -\frac{h}{32}(64h^8 + 96h^7 + 32h^6 - 80h^5 + 52h^4 - 74h^3 + 4h^2 - 18h + 39). \tag{3.7}$$

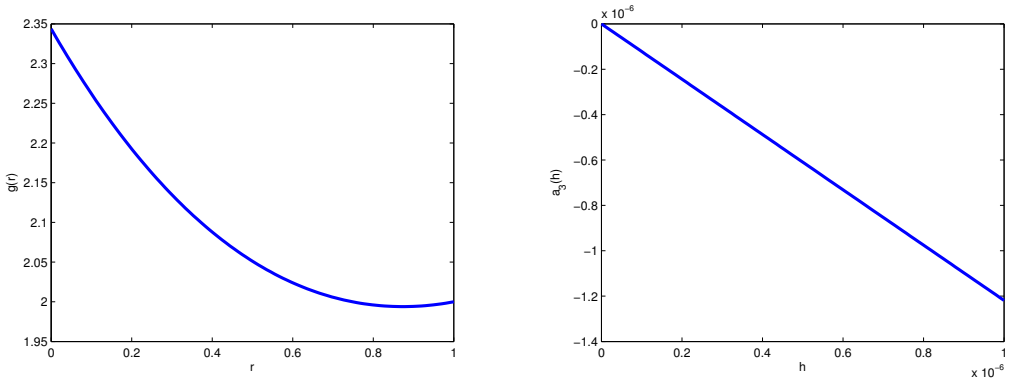

(a) Graph of $g(r) = a_1a_2 - a_3$ for $0 < r < 1$. (b) Values of a_3 for $0 < h < 10^{-6}$.

Figure 1: Verification of the Routh–Hurwitz criteria for the stability of origin.

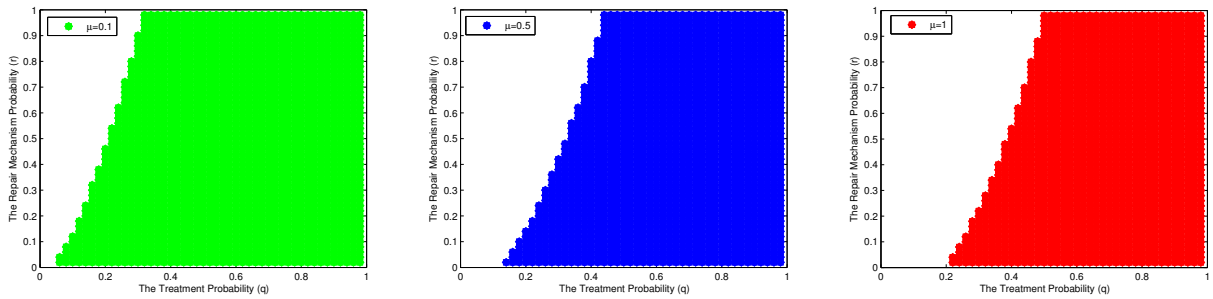

(a) (r, q) region for $\mu = 0.1$. (b) (r, q) region for $\mu = 0.5$. (c) (r, q) region for $\mu = 1$.

Figure 2: (r, q) stability region for the System (3.1) at the origin for $\mu = 0.1$, $\mu = 0.5$ and $\mu = 1$.

According to the Routh-Hurwitz criterion, the System (3.1) is stable at $(0, 0, 0)$ if and only if

$$a_1 > 0, \qquad a_3 < a_1a_2, \qquad a_3 > 0. \tag{3.8}$$

But by using the graph of a_3, we find that $a_3 < 0$ for all $h > 0$ (see Figure 1b) because $a_3(0) = 0$ and $a_3(h)$ is a decreasing function on $[0, 1]$. Hence

$$a_3(h) < 0. \tag{3.9}$$

Therefore, System (3.1) is unstable at the equilibrium point $(0, 0, 0)$. □

The following corollary is a direct result of Theorem 3.3.

Corollary 3.1. *Suppose that S denotes the set of all values q such that System (3.1) is stable at equilibrium point $0 \in \mathbb{R}^3$ corresponding to all $0 < r < 1$. Then*

$$\inf_q S = 0.5. \tag{3.10}$$

Remark 3.2. *As the system is linear and has only one equilibrium point the stability results are global. This stability result plays a crucial role in the treatment as it can be interpreted as the cancer cells population will vanish, which means the radiation therapy is effective.*

3.1.2 Bifurcation analysis

The system parameters stability ranges for cases $\mu = 1$, $\mu = 0.5$, and $\mu = 0.1$ are depicted in Figures 2(a), 2(b), and 2(c), respectively. There are no significant differences observed in the stability regions of the System (3.1) for different values of μ.

Regarding the bifurcation value of the parameter q, we have studied several cases. The value of q is changed with different values of r. The results demonstrate that the system is stable for $q \geq 0.5$ (see Figures 3, 4, and 5).

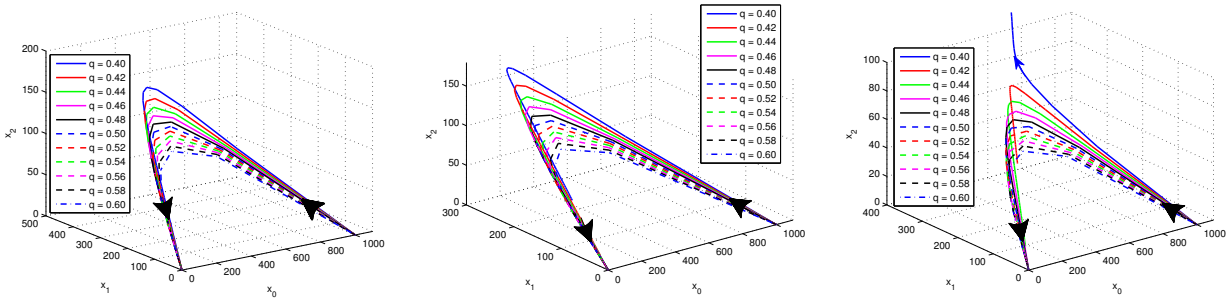

(a) $r = 0.4$ (b) $r = 0.5$ (c) $r = 0.6$

Figure 3: 3-D graph for time-evolution of x_0, x_1, and x_2 where $n_0 = 1000$, q varies from 0.4 to 0.6 with step size 0.05, and $r = 0.4$, $r = 0.5$, and $r = 0.6$.

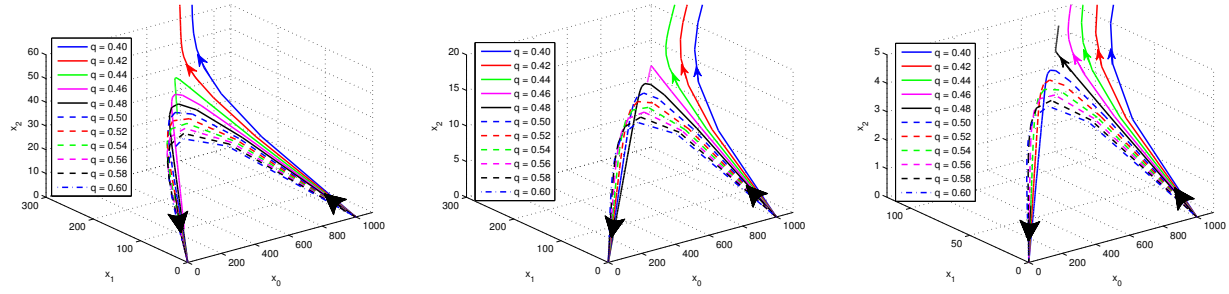

(a) $r = 0.7$ (b) $r = 0.8$ (c) $r = 0.9$

Figure 4: 3-D graph for time-evolution of x_0, x_1, and x_2. where $n_0 = 1000$, q varies from 0.4 to 0.6 with step size 0.05, and $r = 0.7$, $r = 0.8$, and $r = 0.9$.

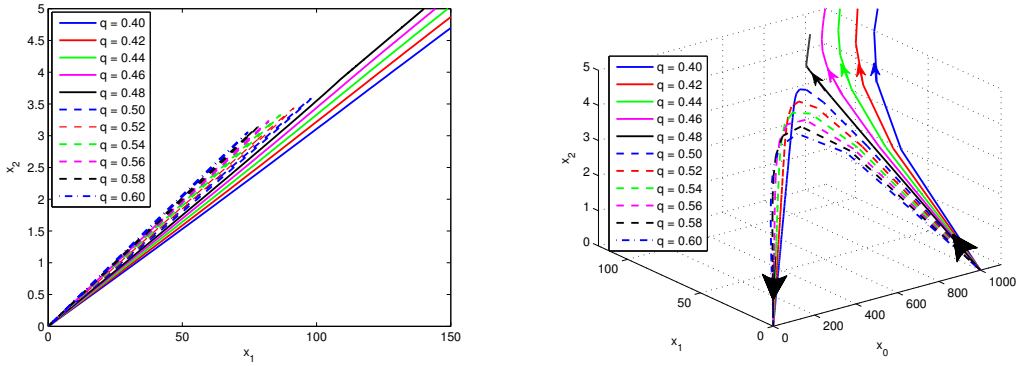

(a) Phase Diagram $x_1 - x_2$. (b) 3D Bifurcation diagram.

Figure 5: Bifurcation analysis: $r = 0.9$ and q varies between 0.4 and 0.6. The system is stable at zero equlibrium when $q \geq 0.5$.

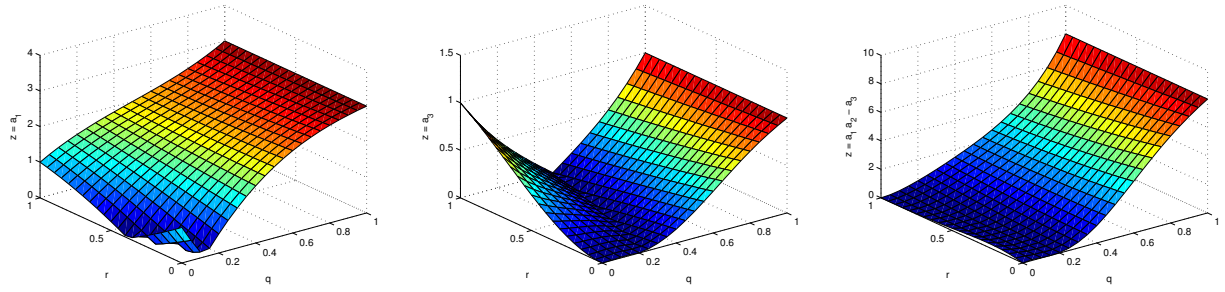

(a) $|a_1(q,r)|$ (b) $|a_1(q,r)a_2(q,r) - a_3(q,r)|$ (c) $|a_3(q,r)|$

Figure 6: 3-D plot for $|a_1(q,r)|$, $|a_1(q,r)a_2(q,r) - a_3(q,r)|$ and $|a_3(q,r)|$. System (3.1) is stable at the origin if and only if these functions are positive.

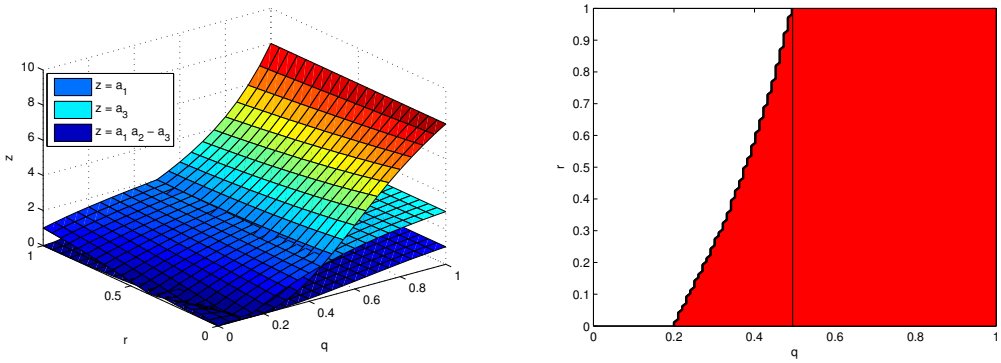

(a) a_1, $a_1a_2 - a_3$ and a_3. (b) The Stability Region.

Figure 7: Intersection of the area in which functions $a_1(q,r)$ and $a_3(q,r)$ are positive and $a_1(q,r)\ a_2(q,r) > a_3(q,r)$. The Routh-Hurwitz Criterion is satisfied for all values of q and r in the blue region.

According to the discussion provided in Section 3.1.1, the system is generally stable when the Routh-Hurwitz criterion is satisfied. In this case, the three conditions of Theorem 3.2 can be represented as 3D graphs with respect to parameters q and r, which are depicted in Figure 6. A stability region is characterized by the intersection of these surfaces, which is illustrated in Figure 7.

3.2 Cells with single-strand breaks and double-strand breaks as one subpopulations

There are several different methods to recognize single-strand breaks (SSB) and double-strand breaks (DSB) such as PCR (polymerase chain reaction), comet, halo, TUNEL (Terminal deoxyribonucleotidyl transferase-mediated deoxyuridine triphosphate nick end labeling) assay, HPLC-Electrospray tandem mass spectrometry, FISH (Fluorescence in situ hybridization), FCM (Flow cytometry), annexin V labeling, immunological assays including immunofluorescent and chemiluminescence thymine dimer detection, immunohistochemical assay, Enzyme-linked immunosorbent assay (ELISA), Radio immunoassay (RIA), Gas chromatography-mass spectrometry, and electrochemical methods (Kumari et al., 2008). The main drawback of these methods is that they are not able to distinguish between SSDs and DSBs. As a result, we can take both populations (DSBs and SSBs) as one subpopulation. Therefore, we can consider $m = 2$, i.e., the tumor population is divided into two subpopulations: cells without DNA fragmentation and cells with DNA fragmentation (SSBs and DSBs).

3.2.1 Stability analysis

Based on Equation (2.6), the matrix A in the System (2.4) is defined as

$$A(q,r) = \begin{bmatrix} 2(q-1)^2 - 2qr(q-1) - 1 & -r(q-1) \\ 2q(q-1)(r-1) & (q-1)(r-1) - 1 \end{bmatrix} \tag{3.11}$$

where $0 \le q, r \le 1$.

Theorem 3.4. *Suppose that the matrix A is defined as Equation (3.11) and $q = 0.5$. Therefore, the System (2.4) is stable at equilibrium point $(0,0)^\top$ for all $0 < r < 1$.*

Proof. For $q = 0.5$

$$A = \begin{bmatrix} \frac{r}{2} - \frac{1}{2} & \frac{r}{2} \\ \frac{1}{2} - \frac{r}{2} & -\frac{r}{2} - \frac{1}{2} \end{bmatrix} \tag{3.12}$$

In addition

$$\lambda_1 + \lambda_2 = -1 \tag{3.13}$$

and

$$\lambda_1 \lambda_2 = \frac{1-r}{4} \tag{3.14}$$

Therefore, for any $0 < r < 1$, the eigenvalues of the matrix A have negative real parts. Hence, the System (2.4) is stable for all $0 < r < 1$. □

3.2.2 Bifurcation analysis

In this section, we will show how the change in parameters of the model is influencing the lifespan. Due to the complexity of the system, most of our results in this section are based on the numerical simulations. Figures 8–10 show the stability region of the system with respect to parameter μ. Figure 8 shows a significant difference among the stability region of the system, for $m = 2$ where $\mu = 0.1$, $\mu = 0.5$, and $\mu = 1$. The same results are shown where $m = 5$ in Figure 9. The difference among stability regions for $m = 10$ is insignificant (depicted in Figure 10). Therefore, it can be inferred that the parameter μ is not an influential parameter when the number of targets is greater than 10.

As seen in Figures 11 and 12, the stability region experiences significant change if the number of targets varies from $m = 4$ to $m = 50$. However, for larger values of m, the stability region is changing slightly (see Figure 12). For instance, stability regions corresponding to $m = 10$ and $m = 20$ are different only in one point. In contrast, the difference in the stability region corresponding to $m = 4$ and $m = 2$ cases is significant. As a result of this study, we can say that for lower values of m the stability area are quite different, while for the higher values of m, the stability areas are the same.

The next parameter of the model is the probability that a cell gives birth after the application of a dose fraction μ. First, we consider $m = 2$, $q = 0.6$. The effect of parameter μ on the tumor lifespan L are shown in Figure 13, in which the initial number of cells varies among $n_0 = 10^3, 10^7$ and 10^{10}. The blue and red solid lines show the tumor lifespan, when the parameter $0 \le r \le 1$ corresponding to $\mu = 0.1$ and $\mu = 1$, respectively.

Now, suppose that $q = 0.6$, $n_0 = 10^7$ and $\mu = 1$. Figure 14 represents the influence of parameter m on the tumor lifespan L. The blue and red solid lines are corresponding to the values $\mu = 0.1$ and $\mu = 1$ in which m changes among 3, 5 and 7. As seen, the tumor lifespan corresponds to different values of μ that are almost the same if m is large enough (for instance $m = 7$).

For fixed values of $q = 0.8$, and $n_0 = 10^3$, the tumor lifespan remains unchanged for $m = 2$ and $m = 3$ (see Figure 15). In addition, for $m = 6$, and $m = 7$, the changes in the tumor lifespan are insignificant (see Figure 16). However, a big gap in the tumor lifespan is visible, for $m = 2$, $m = 7$, and $0.3 \le r \le 1$.

As seen in Figures 15 and 16, the lifespan corresponding to the values of $q = 0.8$, and $m = 2$ is fairly similar to the tumor lifespan associated with $q = 0.9$, and $m = 7$. This shows that, although the repair mechanism (r) and the number of a cell's target (m) are important in this model, controlling the parameter (q) is the most important fact.

Now, suppose that $m = 2$, and $n_0 = 10^3$. For low, middle, and high values of the repair mechanism probability, if $q = 0.5$, the tumor lifespan changes between 30 and 130. However, for $q \ge 0.6$, the changes in the values of repair mechanism parameter (r) affect the tumor lifespan insignificantly (see Figure 17).

Suppose that $m = 2$, and $n_0 = 10^3$. However, the System (2.4) is stable when $q = 0.5$; this value of (q) is not suitable (see Figure 18). In addition, the tumor lifespan is stabilized and constant for $q = 0.6$ and $q = 0.8$, respectively.

Finally, it is clear that the treatment parameter (q) is more important than the repair mechanism parameter (r) because if we can control the treatment parameter in an acceptance range of $0.8 \le q \le 1$ then the tumor lifespan will be stabilized for any value of the repair mechanism value r. As a result, the treatment process will be more effective.

Table 1 shows the change of the tumor lifespan (L) for a fixed value of $n_0 = 10^3$ and a small value of r ($r = 0.3$) corresponding to the different values of parameters q and m. The tumor lifespan is clearly stabilized when $q \ge 0.8$.

In contrast, Table 2 shows the variation in tumor lifespan for a fixed value of $n_0 = 10^3$ and large value of r ($r = 0.9$) and different values of parameters q and m. As seen before, $q = 0.5$ is not a suitable value for the treatment parameter. In Figures 19 and 20 the 3-D simulation of the tumor lifespan for $q \ge 0.6$, and $0 \le r < 1$ for two values $m = 2$, $m = 6$ are represented, respectively. Moreover, we compare the values of L corresponding to different values of $0.6 \le q \le 1$ and $0 \le r \le 1$ for $m = 2$ and $m = 6$ in Figure 21. Finally, 3-D stability region of the System (2.4) where $m = 2, 5$ and $m = 10, 20$ and $\mu = 1$ in Figures 22 and 23, respectively.

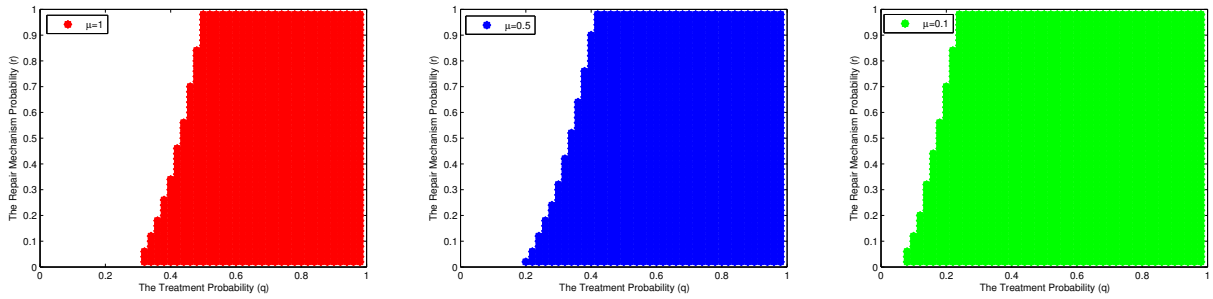

(a) $\mu = 1$ (b) $\mu = 0.5$ (c) $\mu = 0.1$

Figure 8: (r, q) stability region at zero equilibrium for $m = 2$.

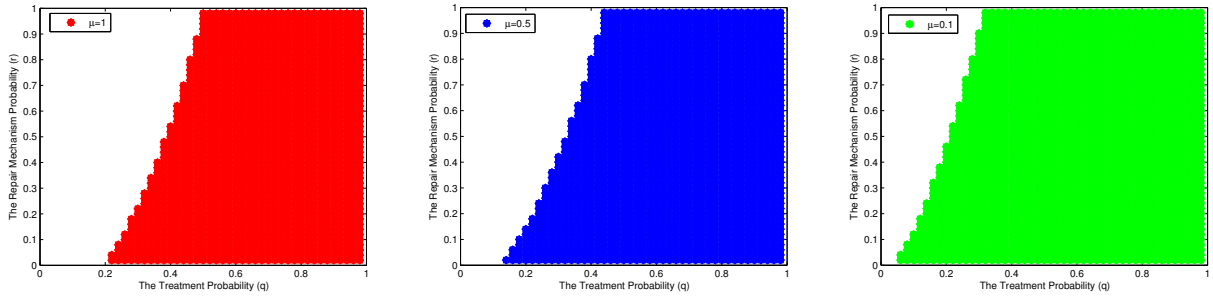

(a) $\mu = 1$ (b) $\mu = 0.5$ (c) $\mu = 0.1$

Figure 9: (r, q) stability region at zero equilibrium for $m = 5$.

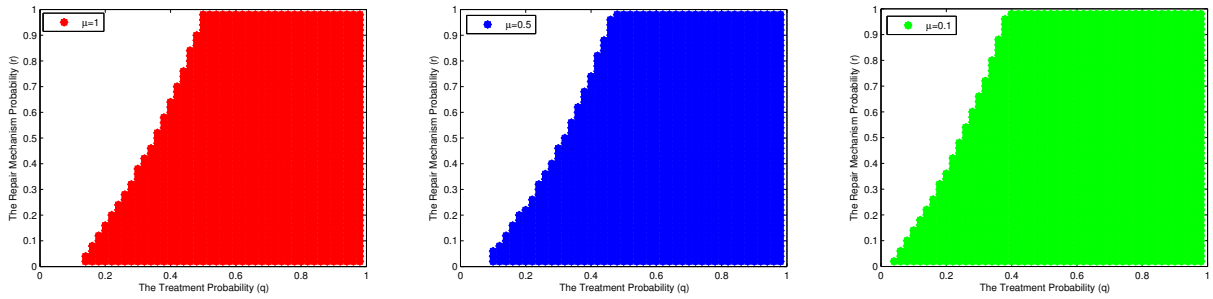

(a) $\mu = 1$ (b) $\mu = 0.5$ (c) $\mu = 0.1$

Figure 10: (r, q) stability region at zero equilibrium for $m = 10$.

Table 1: Influence of the parameters q, m on the Tumor Lifespan L, where $n_0 = 10^3$ and $r = 0.3$.

	$q = 2$	$q = 3$	$q = 4$	$q = 5$	$q = 6$	$q = 7$
$m = 0.6$	18	18	21	24	28	33
$m = 0.7$	13	14	15	17	19	21
$m = 0.8$	11	11	12	13	14	15
$m = 0.9$	9	9	10	10	10	11

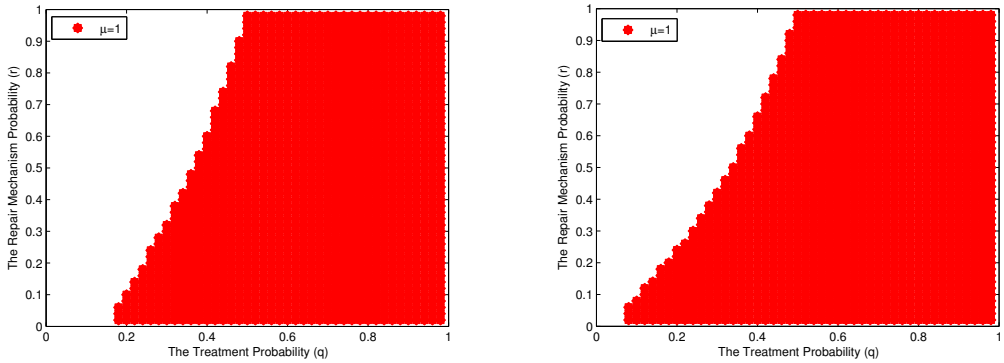

(a) $m = 4$ (b) $m = 10$

Figure 11: Stability Region at zero equilibrium for $m = 4$ and $m = 10$.

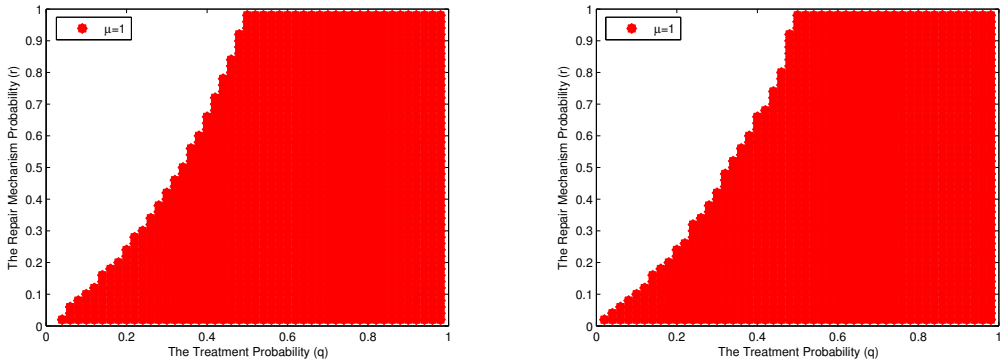

(a) $m = 20$ (b) $m = 50$

Figure 12: Stability Region at zero equilibrium for $m = 20$ and $m = 50$.

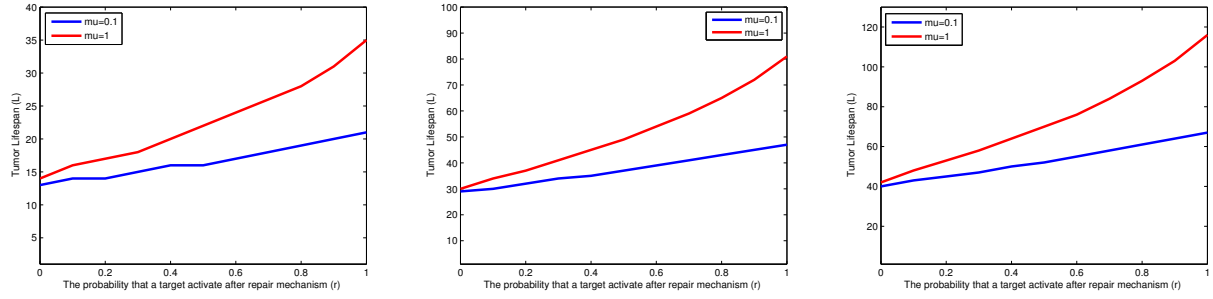

(a) $n_0 = 10^3$ (b) $n_0 = 10^7$ (c) $n_0 = 10^{10}$

Figure 13: Influence of μ on the tumor lifespan for $m = 2$.

Table 2: Influence of the parameters q, m on the Tumor Lifespan L, where $n_0 = 10^3$ and $r = 0.9$.

	$q = 2$	$q = 3$	$q = 4$	$q = 5$	$q = 6$	$q = 7$
$m = 0.6$	31	39	54	81	124	193
$m = 0.7$	17	21	27	54	50	69
$m = 0.8$	12	14	16	27	24	30
$m = 0.9$	9	10	11	16	13	14

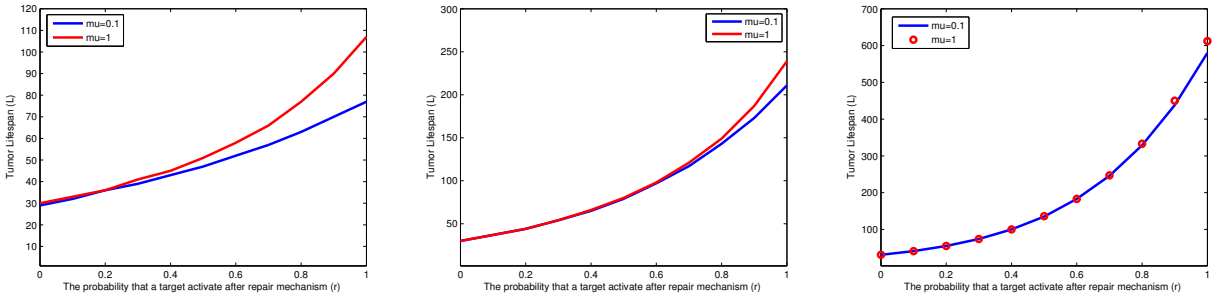

(a) $m = 3$ (b) $m = 5$ (c) $m = 7$

Figure 14: Influence of μ on the tumor lifespan for $q = 0.6$ and $n_0 = 10^7$.

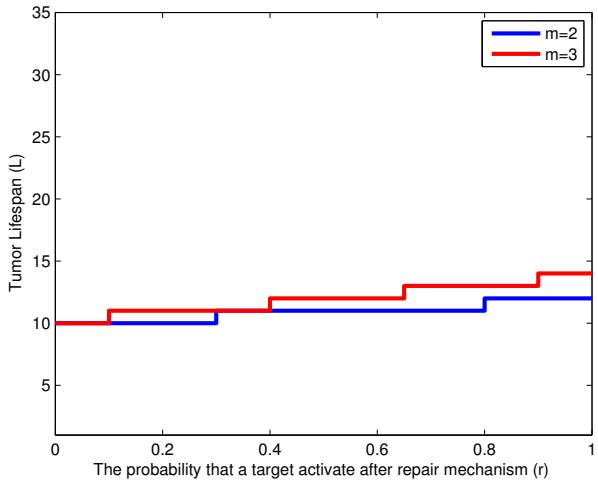

Figure 15: Compare the lifespan trend for $m = 2$ and $m = 3$, where $q = 0.8$ and $n_0 = 10^3$.

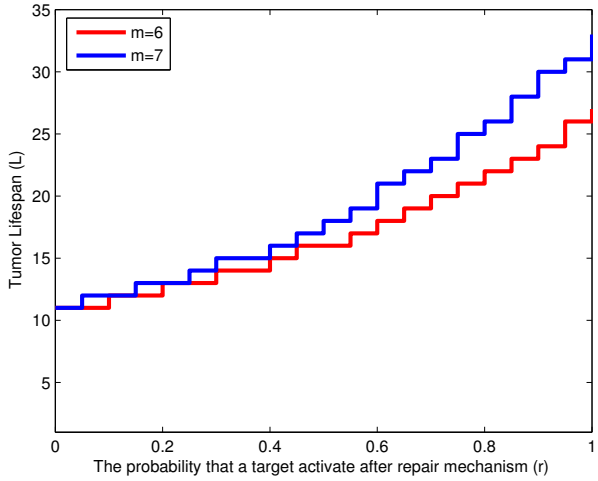

Figure 16: Compare the lifespan trend for $m = 6$ and $m = 7$, where $q = 0.9$ and $n_0 = 10^3$.

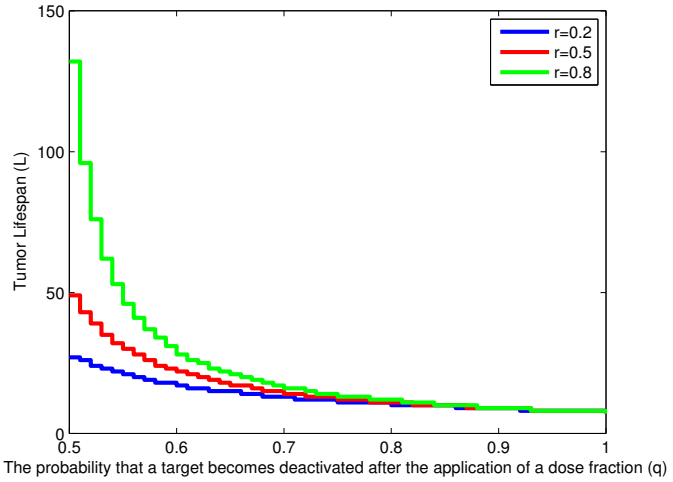

Figure 17: The influence of the repair mechanism probability (r) on the tumor lifespan where $m = 2$ and $n_0 = 10^3$.

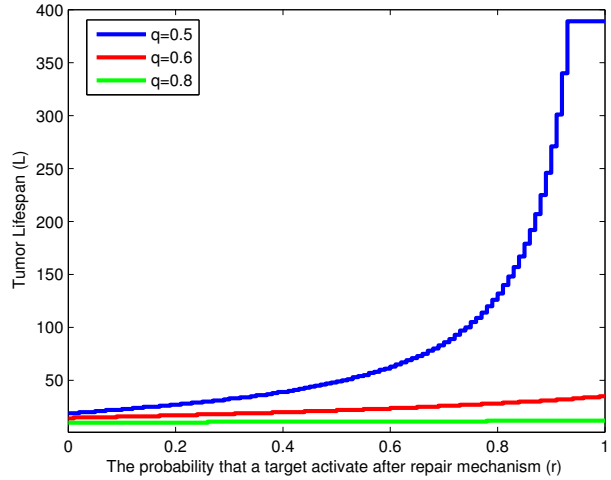

Figure 18: The influence of the treatment probability (q) on the tumor lifespan where $m = 2$ and $n_0 = 10^3$.

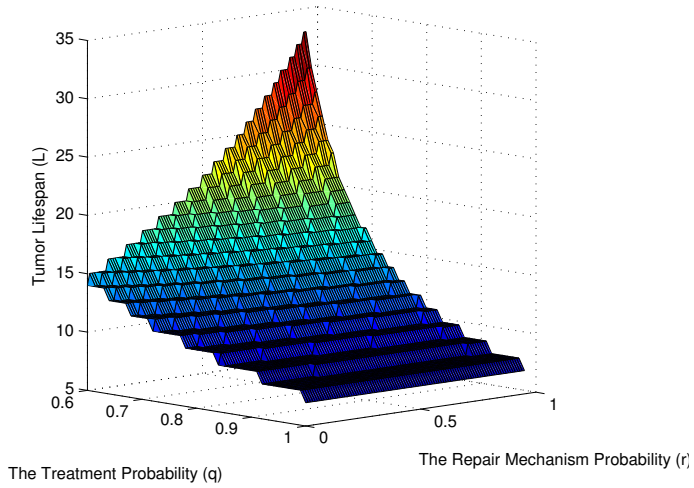

Figure 19: The tumor Lifespan where $m = 2$, $n_0 = 10^3$, $0.6 \leq q \leq 1$, and $0 \leq r \leq 1$.

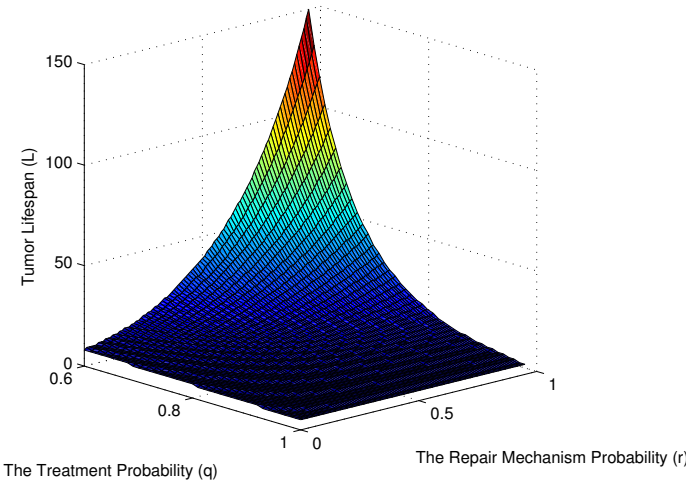

Figure 20: The tumor Lifespan where $m = 6$, $n_0 = 10^3$, $0.6 \leq q \leq 1$, and $0 \leq r \leq 1$.

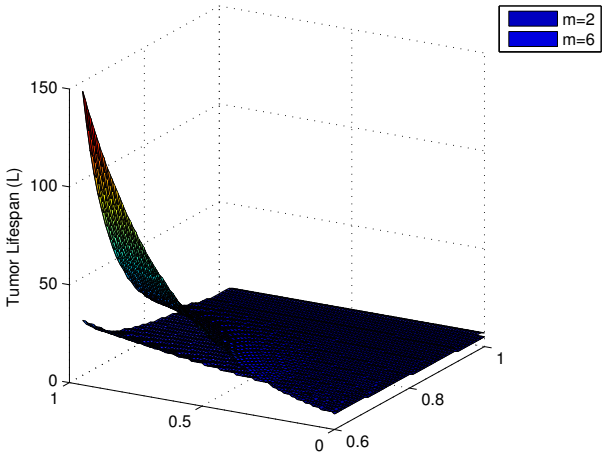

Figure 21: Comparing the tumor lifespan where $m = 2$ and $m = 6$.

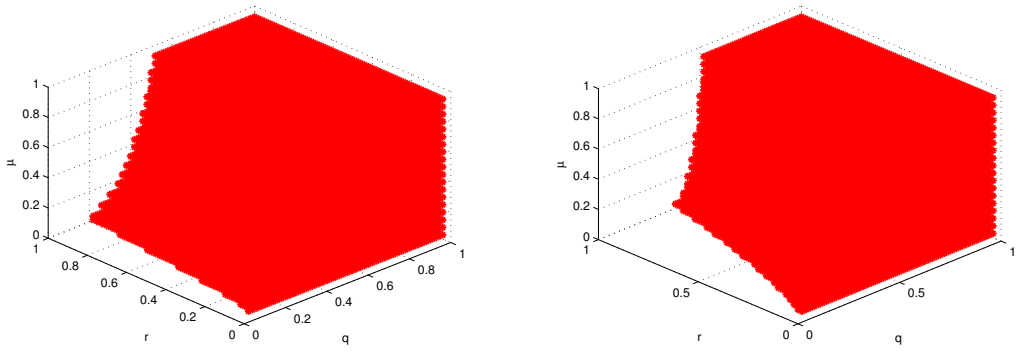

(a) $m = 2$ (b) $m = 5$

Figure 22: 3-D stability region.

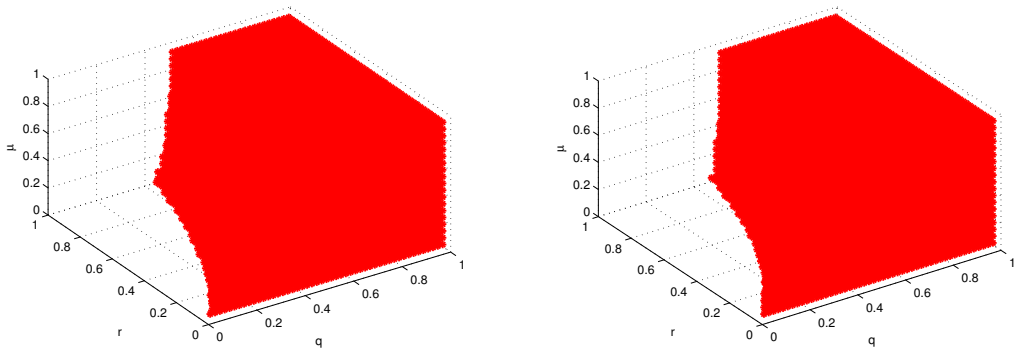

(a) $m = 10$ (b) $m = 20$

Figure 23: 3-D stability region.

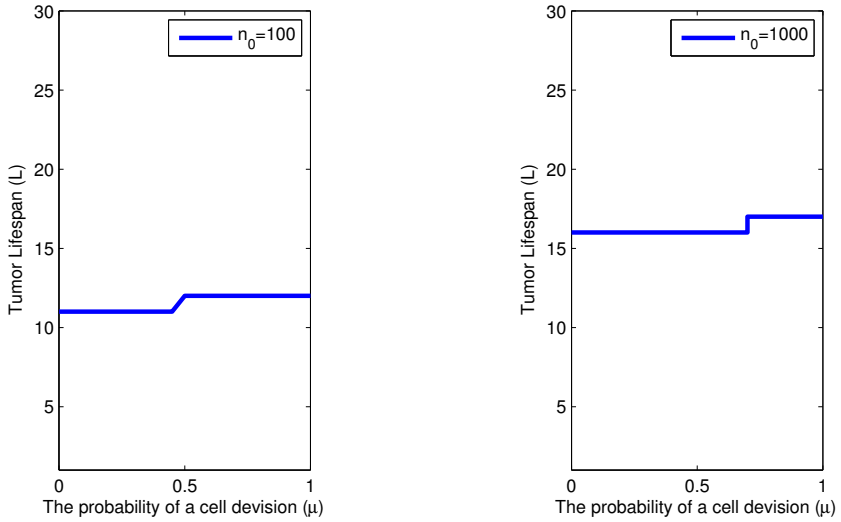

(a) $n_0 = 100$ (b) $n_0 = 1000$

Figure 24: The influence of parameter μ on tumor lifespan for $q = 0.6$ and $r = 0.2$.

3.3 Numerical analysis on the tumor lifespan

In this section, we study the influence that system parameters have on the tumor lifespan and also provide a numerical bifurcation analysis of the System (3.1). This is a linear system with three parameters, q, r, and n_0. The numerical simulations were carried out using the MATLAB software package. Based on the tumor lifespan definition provided in Equation (2.3), we demonstrate that parameter q has the highest impact on the lifespan. Figure 24 shows the effect of parameter μ on the tumor lifespan for $r = 0.2$, which is similar to the result of Keinj et al. (2012). Figure 25 depicts the effect of parameter μ on the tumor lifespan for different initial condition values: $n_0 = 10^3$, 10^7 and 10^{10}. The blue solid line and red dash line represent the tumor lifespan corresponding to $\mu = 0.1$ and $\mu = 1$, respectively. In this case, it is clear that when μ changes from 0.1 to 1, there is a slight change in tumor lifespan L.

Table 3 shows the variation in the tumor lifespan for the fixed value of $n_0 = 100$ and different values of parameters q and r. The tumor lifespan is clearly stabilized for $q \geq 0.8$.

These results emphasize that the effect of parameter q on the tumor lifespan is more dominant than the other parameters (see Figure 26). In addition, corresponding to the fixed parameter value $q = 0.9$, the tumor lifespan changes are insignificant for $0 < r < 1$ and $10^2 < n_0 < 10^5$ (see Table 4). The variations in tumor lifespan (L) with respect to the changes in the initial tumor cell numbers, n_0, are depicted in Figure 27 and are in very good agreement with the results of Keinj et al. (2012).

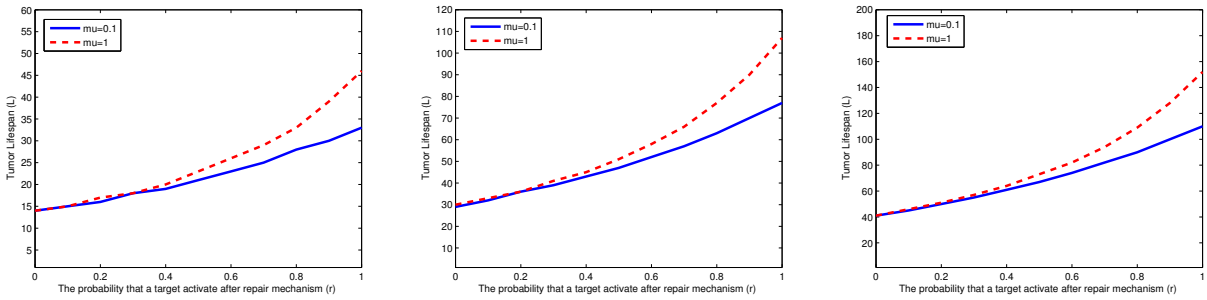

(a) $n_0 = 10^3$ (b) $n_0 = 10^7$ (c) $n_0 = 10^{10}$

Figure 25: Influence of μ on tumor lifespan where n_0 changes from 10^3 to 10^{10} when $q = 0.6$ and $0 < r < 1$.

Table 3: Influence of parameters (q) and (r) on the tumor lifespan (L) for $n_0 = 100$.

	$r = 0.1$	$r = 0.2$	$r = 0.3$	$r = 0.4$	$r = 0.5$	$r = 0.6$	$r = 0.7$	$r = 0.8$
$q = 0.5$	14	16	19	23	28	36	50	77
$q = 0.6$	11	12	13	14	16	17	20	23
$q = 0.7$	9	9	10	10	11	11	12	13
$q = 0.8$	7	8	8	8	8	8	9	9
$q = 0.9$	6	6	6	6	7	7	7	7

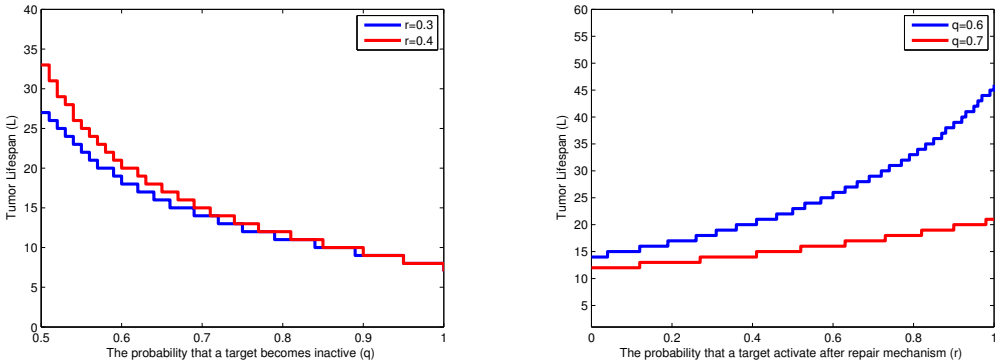

(a) interactivation probabililities (q) (b) reactivation probabilities (r)

Figure 26: Influence of inactivation (q) and reactivation probabilities (r) on tumor lifespan (L).

Table 4: Tumor lifespan for $q = 0.9$ when n_0 varies between 10^2 and 10^5.

	$r = 0.1$	$r = 0.2$	$r = 0.3$	$r = 0.4$	$r = 0.5$	$r = 0.6$	$r = 0.7$	$r = 0.8$
$n_0 = 10^2$	6	6	6	6	7	7	7	7
$n_0 = 10^3$	9	9	9	9	9	10	10	10
$n_0 = 10^4$	12	12	12	12	12	12	13	13
$n_0 = 10^5$	14	15	15	15	15	15	16	16

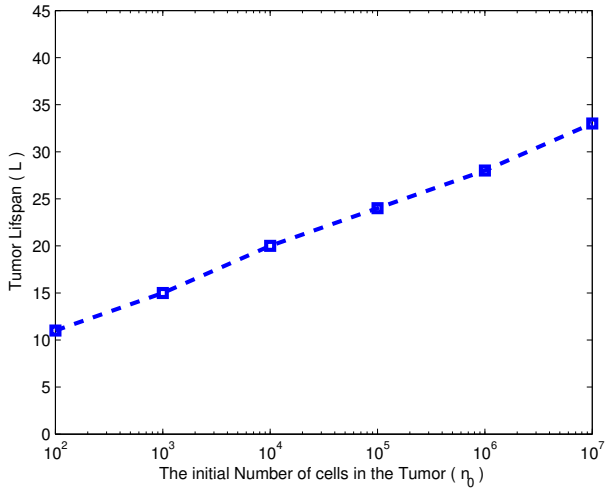

Figure 27: Variations in tumor lifespan (L) with respect to changes in the initial number of tumor cells (n_0) for $r = 0.1$ and $q = 0.5$.

4 Discussion

In this paper, we have proposed a hybrid differential equations model for the evolution of single and double strand breaks in the treatment by radiotherapy. The proposed model comprises the dynamics of a tumor cell population due to the effect of the treatment on cells through each cell's reaction to radiation. For instance, after applying the first dose fraction and after the repair mechanism, a cell may remain in subpopulation x_0 or move to other sub-populations, x_i, $i = 1, \ldots, (m-1)$, or it may die. Therefore, the cells' reaction to treatment is different in this model and can be interpreted as heterogeneity. Using this model, we confirmed that the treatment effect parameter q has a more important role than the repair mechanism parameter r. We have demonstrated that $q = 0.5$ is a the bifurcation value, which results in the stability of the System (3.1) for all $0 < r < 1$. We showed that the death rate of subpopulation x_i has less impact than that of subpopulation x_j when $i < j$, which means that cells with j deactivated targets are more radiosensitive than cells with i deactivated targets. Therefore, damaged cells are unable to resist radiation, which is in complete agreement with evidence provided by Keinj et al. (2011) and by Keinj et al. (2012). The model also presents formula for the tumor lifespan.

5 Conclusion

In this study, the population dynamics of tumor cells in the process of radiotherapy was studied. A system of differential equations with random variable coefficients was introduced to capture the heterogeneity of cell damage and the repair mechanism between two consecutive dose fractions. The effect of radiation in the case of single-strand and double-strand breaks was considered as a special instance of the model when $m = 3$ and $m = 2$. Moreover, the stability of this system was assessed both analytically and numerically, when each cell contains two and three targets ($m = 3$, $m = 2$). Based on the tumor lifespan, the effects of the probability that a target will be inactive after a dose fraction q and the probability that a target will reactivate after the repair mechanism r were investigated numerically. Our results are in good agreement with previous results presented by Keinj et al. (2012).

Acknowledgments

The first author appreciates Dr. Ivy Chung and Dr. Ung Ngie Min from Faculty of Medicine, University of Malaya and Prof. Fazlul Sarkar from School of Medicine, Wayne State University for their constructing comments with regard to the manuscript. The third author thanks Dr. Eric Van Dornshuld from Mississippi State University.

References

Adam, J. and N. Bellomo (2012). *A survey of models for tumor-immune system dynamics*. Springer Science & Business Media. 141

Araujo, R. P. and D. S. McElwain (2004). A history of the study of solid tumour growth: the contribution of mathematical modelling. *Bulletin of mathematical biology 66*(5), 1039–1091. 141

Bajzer, Z., M. Marušić, and S. Vuk-Pavlović (1996). Conceptual frameworks for mathematical modeling of tumor growth dynamics. *Mathematical and computer modelling 23*(6), 31–46. 141

Bellomo, N. and M. Delitala (2008). From the mathematical kinetic, and stochastic game theory to modelling mutations, onset, progression and immune competition of cancer cells. *Physics of Life Reviews 5*(4), 183–206. 141

Bellomo, N., N. Li, and P. K. Maini (2008). On the foundations of cancer modelling: selected topics, speculations, and perspectives. *Mathematical Models and Methods in Applied Sciences 18*(04), 593–646. 141

Bellomo, N. and L. Preziosi (2000). Modelling and mathematical problems related to tumor evolution and its interaction with the immune system. *Mathematical and Computer Modelling 32*(3), 413–452. 141

Byrne, H., T. Alarcon, M. Owen, S. Webb, and P. Maini (2006). Modelling aspects of cancer dynamics: a review. *Philosophical Transactions of the Royal Society of London A: Mathematical, Physical and Engineering Sciences 364*(1843), 1563–1578. 141

Chaplain, M. A. (2008). Modelling aspects of cancer growth: insight from mathematical and numerical analysis and computational simulation. In *Multiscale Problems in the Life Sciences*, pp. 147–200. Springer. 141

Cohen, L. (1971). A cell population kinetic model for fractionated radiation therapy 1: I. normal tissues. *Radiology 101*(2), 419–427. 142

Coppel, W. (1965). *Stability and asymptotic behavior of differential equations*. Heath. 144

Dullens, H., M. Van Der Tol, R. De Weger, and W. Den Otter (1986). A survey of some formal models in tumor immunology. *Cancer Immunology, Immunotherapy 23*(3), 159–164. 141

Ellis, F. (1969). Dose, time and fractionation: a clinical hypothesis. *Clinical Radiology 20*(1), 1–7. 142

Gompertz, B. (1825). On the nature of the function expressive of the law of human mortality, and on a new mode of determining the value of life contingencies. *Philosophical transactions of the Royal Society of London 115*, 513–583. 141

Joiner, M. and A. van der Kogel (2009). Basic clinical radiobiology. *Basic Clinical Radiobiology. 4th ed2009*. 142

Keinj, R., T. Bastogne, and P. Vallois (2011). Multinomial model-based formulations of tcp and ntcp for radiotherapy treatment planning. *Journal of Theoretical Biology 279*(1), 55–62. 142, 143, 156

Keinj, R., T. Bastogne, and P. Vallois (2012). Tumor growth modeling based on cell and tumor lifespans. *Journal of theoretical biology 312*, 76–86. 154, 156

Khoronenkova, S. V. and G. L. Dianov (2015). Atm prevents dsb formation by coordinating ssb repair and cell cycle progression. *Proceedings of the National Academy of Sciences 112*(13), 3997–4002. 142

Kumari, S., R. P. Rastogi, K. L. Singh, S. P. Singh, and R. P. Sinha (2008). Dna damage: detection strategies. *EXCLI J 7*, 44–62. 147

Martins, M., S. Ferreira, and M. Vilela (2007). Multiscale models for the growth of avascular tumors. *Physics of Life Reviews 4*(2), 128–156. 141

Nagy, J. D. (2005). The ecology and evolutionary biology of cancer: a review of mathematical models of necrosis and tumor cell diversity. *Mathematical biosciences and engineering: MBE 2*(2), 381–418. 141

Ohnishi, T., E. Mori, and A. Takahashi (2009). Dna double-strand breaks: their production, recognition, and repair in eukaryotes. *Mutation Research/Fundamental and Molecular Mechanisms of Mutagenesis 669*(1), 8–12. 142

Oroji, A., M. Omar, and S. Yarahmadian (2016). An ito stochastic differential equations model for the dynamics of the mcf-7 breast cancer cell line treated by radiotherapy. *Journal of theoretical biology 407*, 128–137. 141, 143

Oroji, A., S. Yarahmadian, S. Seddighi, and M. Omar (2018). A mathematical model for tumor cell population dynamics based on target theory and tumor lifespan. *arXiv preprint arXiv:1801.07113*. 142, 143

Piantadosi, S., J. B. Hazelrig, and M. E. Turner (1983). A model of tumor growth based on cell cycle kinetics. *Mathematical biosciences 66*(2), 283–306. 141

Roose, T., S. J. Chapman, and P. K. Maini (2007). Mathematical models of avascular tumor growth. *Siam Review 49*(2), 179–208. 141

Sachs, R., L. Hlatky, and P. Hahnfeldt (2001). Simple ode models of tumor growth and anti-angiogenic or radiation treatment. *Mathematical and Computer Modelling 33*(12), 1297–1305. 141

Vilenchik, M. M. and A. G. Knudson (2000). Inverse radiation dose-rate effects on somatic and germ-line mutations and dna damage rates. *Proceedings of the National Academy of Sciences 97*(10), 5381–5386. 142